ARTICLE

BIOTECHNOLOGY and BIOENGINEERING

Reference and Counter Electrode Positions Affect Electrochemical Characterization of Bioanodes in Different Bioelectrochemical Systems

Fang Zhang,[1] Jia Liu,[1] Ivan Ivanov,[1] Marta C. Hatzell,[1] Wulin Yang,[1] Yongtae Ahn,[1,2] Bruce E. Logan[1]

[1]Department of Civil and Environmental Engineering, Penn State University, 212 Sackett Building, University Park, Pennsylvania 16802; telephone: +1-814-863-7908; fax: +1-814-863-7304; e-mail: blogan@psu.edu

[2]Department of Energy Engineering, Gyeongnam National University of Science and Technology, Dongjin-ro 33, Jinju, Gyeongnam 660-758, Korea

ABSTRACT: The placement of the reference electrode (RE) in various bioelectrochemical systems is often varied to accommodate different reactor configurations. While the effect of the RE placement is well understood from a strictly electrochemistry perspective, there are impacts on exoelectrogenic biofilms in engineered systems that have not been adequately addressed. Varying distances between the working electrode (WE) and the RE, or the RE and the counter electrode (CE) in microbial fuel cells (MFCs) can alter bioanode characteristics. With well-spaced anode and cathode distances in an MFC, increasing the distance between the RE and anode (WE) altered bioanode cyclic voltammograms (CVs) due to the uncompensated ohmic drop. Electrochemical impedance spectra (EIS) also changed with RE distances, resulting in a calculated increase in anode resistance that varied between 17 and 31 Ω (−0.2 V). While WE potentials could be corrected with ohmic drop compensation during the CV tests, they could not be automatically corrected by the potentiostat in the EIS tests. The electrochemical characteristics of bioanodes were altered by their acclimation to different anode potentials that resulted from varying the distance between the RE and the CE (cathode). These differences were true changes in biofilm characteristics because the CVs were electrochemically independent of conditions resulting from changing CE to RE distances. Placing the RE outside of the current path enabled accurate bioanode characterization using CVs and EIS due to negligible ohmic resistances (0.4 Ω). It is therefore concluded for bioelectrochemical systems that when possible, the RE should be placed outside the current path and near the WE, as this will result in more accurate representation of bioanode characteristics.

Correspondence to: B.E. Logan
Contract grant sponsor: Award KUS-I1-003-13 from the King Abdullah University of Science and Technology (KAUST)
Received 7 December 2013; Revision received 11 March 2014; Accepted 27 March 2014
Accepted manuscript online 12 April 2014;
Article first published online 16 June 2014 in Wiley Online Library (http://onlinelibrary.wiley.com/doi/10.1002/bit.25253/abstract).
DOI 10.1002/bit.25253

Biotechnol. Bioeng. 2014;111: 1931–1939.

KEYWORDS: bioelectrochemical systems; bioanode; uncompensated ohmic drop; reference electrode placement; electrochemical impedance spectroscopy; cyclic voltammetry

Introduction

Bioelectrochemical systems (BESs) represent promising approaches for the sustainable recovery of valued resources from waste streams (Logan and Rabaey, 2012). In BESs, exoelectrogenic bacteria oxidize organic matter and donate electrons to the anode (Lovley, 2006), while different electron acceptors can be reduced biologically or abiotically at the cathode depending on the purpose of the system (Logan and Rabaey, 2012; Lovley, 2008). Air cathode microbial fuel cells (MFCs) are one type of BES that use oxygen as the final electron acceptor, and convert chemical energy directly to electrical power (Logan et al., 2006). In order to reduce internal resistances of MFCs, and increase electrode packing densities, a separator electrode assembly (SEA) configuration which closely places the electrodes on either side of a separator, has been proposed to minimize electrode spacing (Zhang et al., 2013). This SEA configuration has improved power production and coulombic efficiencies compared to configurations with more widely spaced electrode (SPA) configurations (Chen et al., 2013; Fan et al., 2007).

Improvement in BES performance requires accurate characterization of electrode performance in these different configurations. To accomplish this, a potentiostat is used with a three-electrode setup consisting of a working electrode (WE), a counter electrode (CE), and a reference electrode (RE). This setup enables characterization of a single electrode separated from the contributions of other components to

the total impedance of the cell (He and Mansfeld, 2009; He et al., 2006; Marsili et al., 2008). The RE is needed to set the potential of the WE in order to accurately characterize the WE performance. To properly function, the RE must be placed in ionic contact with the same electrolyte as the WE. In order to ensure a constant RE potential, and produce an accurate WE set potential, current should not be drawn from the RE. The electrolyte used in BESs can have high inherent resistance (IR) due to the need to maintain low ionic strength solutions for the exoelectrogenic microorganisms on the anode. A high electrolyte resistance can result in deviations in the applied potential relative to the set potential, as a result of the potential losses produced by the solution (i.e., IR drop). This uncompensated IR drop is affected by the distribution of the total current flow between the WE and the CE, and therefore it is affected by the reactor configuration and the electrode positioning (Bard and Faulkner, 2001; Hack et al., 1990).

While BESs present unique challenges relative to RE and WE placement, the importance of the location of these electrodes is not limited to biological systems (Hack et al., 1990). The electrochemical characterization of thin solid electrolyte fuel cells, for example, showed that results were RE position dependent and prone to errors (Fiaud et al., 1987; Hsieh et al., 1997; Piela et al., 2007; Winkler et al., 1998; Zeng et al., 2010). When the RE is placed in a region of non-uniform current density, the RE can possibly sample a range of equipotential surfaces, resulting in the discrepancies in the measurements (Hsieh et al., 1997). The frequency dependent equipotential line shift will also contribute errors to the impedance measurements (Winkler et al., 1998). So far, the RE placement and IR errors have received insufficient attention in BES studies.

Different reactor configurations and electrode geometries have been used in BES studies, making it nearly impossible to maintain the same positions of the three-electrode setup in these different reactors due to the geometrical constraints. For example, in the SEA configuration, the RE cannot fit in between the two electrodes due to a lack of sufficient space. The use of electrodes with different shapes such as rods, brushes, tubular, and flat plates (Logan et al., 2007; Rabaey et al., 2005) also affects the current distribution and thus the IR drop in the electrochemical tests. This IR drop may not only introduce errors in the measurements electrochemically, but also can result in biological changes in the bioanodes. When anodes in MFCs were acclimated to different set anode potentials they showed differences in startup time, power production, and electrochemical performance (Sun et al., 2012; Torres et al., 2009; Wang et al., 2009; Zhang et al., 2013; Zhu et al., 2013), likely due to the selection of different bacteria species with different anode potentials during the acclimation. Even with pure cultures the set potential can alter expression of different electron transport systems, thus affecting the actual reactions (Dumas et al., 2008; Wei et al., 2010). These changes in the electrochemical behavior or composition of the microorganisms are much different than that of abiotic electrochemical systems where the reaction pathways and potentials are not altered. Therefore, accurate setting and measurement of bioanode potentials is very important, particularly during reactor acclimation. In reactors with different configurations and electrode geometries, the IR drop may affect the actual applied potential to a different extent depending on its placement and reactor configuration. This altered anode potential could be a contributing factor in the inconsistent results on optimal set potentials reported in different studies (Wagner et al., 2010).

In this study, we evaluated the impact of reactor configuration and the positions of the RE and CE on the electrochemical characterization of anodes using SPA and SEA configurations. Anodes were examined using electrochemical impedance spectroscopy (EIS) and cyclic voltammetry (CV), as a function of RE and CE positions. The effect of IR compensation on the CV tests was also examined with various distances between the WE and the RE.

Materials and Methods

MFC Construction and Operation

MFCs were constructed from cubic-shaped segments, each having a cylindrical anode chamber 2 cm long and 3 cm in diameter (Liu and Logan, 2004). The anodes were graphite fiber brushes that were heat-treated at 450°C for 30 min, which previously showed better oxygen tolerance and long-term stability than the flat anode material in the SEA configuration (Hays et al., 2011). Cathodes were made of carbon cloth as previously described (Cheng et al., 2006), with a diffusion layer made of PTFE on the air facing side, and a catalyst layer (Pt, 0.5 mg cm^{-2}) on the solution side.

Reactors were inoculated with the effluent from an MFC operated for over 1 year, and fed an sodium acetate medium (1.0 g L^{-1}) that contained a phosphate buffer solution (PBS; 50 mM; Na_2HPO_4 4.58 g L^{-1}, $NaH_2PO_4\,H_2O$ 2.45 g L^{-1}, NH_4Cl 0.31 g L^{-1}, KCl 0.13 g L^{-1}; conductivity of 6.86 ms cm^{-1}), and trace mineral (12.5 mL L^{-1}) and vitamin (5 mL L^{-1}) solutions. Reactors were operated with 1,000 Ω external resistance, in triplicate at 30°C.

Several different configurations were used to examine the effect of different electrode positions and reactor geometry on electrochemical characterization of the bioanodes. Anodes were placed horizontally in the MFC cylindrical chamber with the brush core 0.5 cm from one cube edge. In the SPA-3 MFCs, reactors were constructed using three 2 cm-cube segments with the two electrodes placed at the two ends. The cathode was 5.5 cm away from the anode brush core (Fig. 1A). The SEA-3 similarly had three segments, but the cathode was placed 0.5 cm away from the anode brush core, with two layers of a porous cloth separator (DuPont Sontara, style 8864, Wilmington, DE) used to prevent electrode short circuiting (Fig. 1B). The RE (Bioanalytical Systems, Inc., RE-5B, West Lafayette, IN; +0.209 V vs. a standard hydrogen electrode, SHE) was inserted through the middle hole of the 2 cm-cube segment, so that the RE had three candidate positions of 1 (nearest to the anode, 0.5 cm horizontal

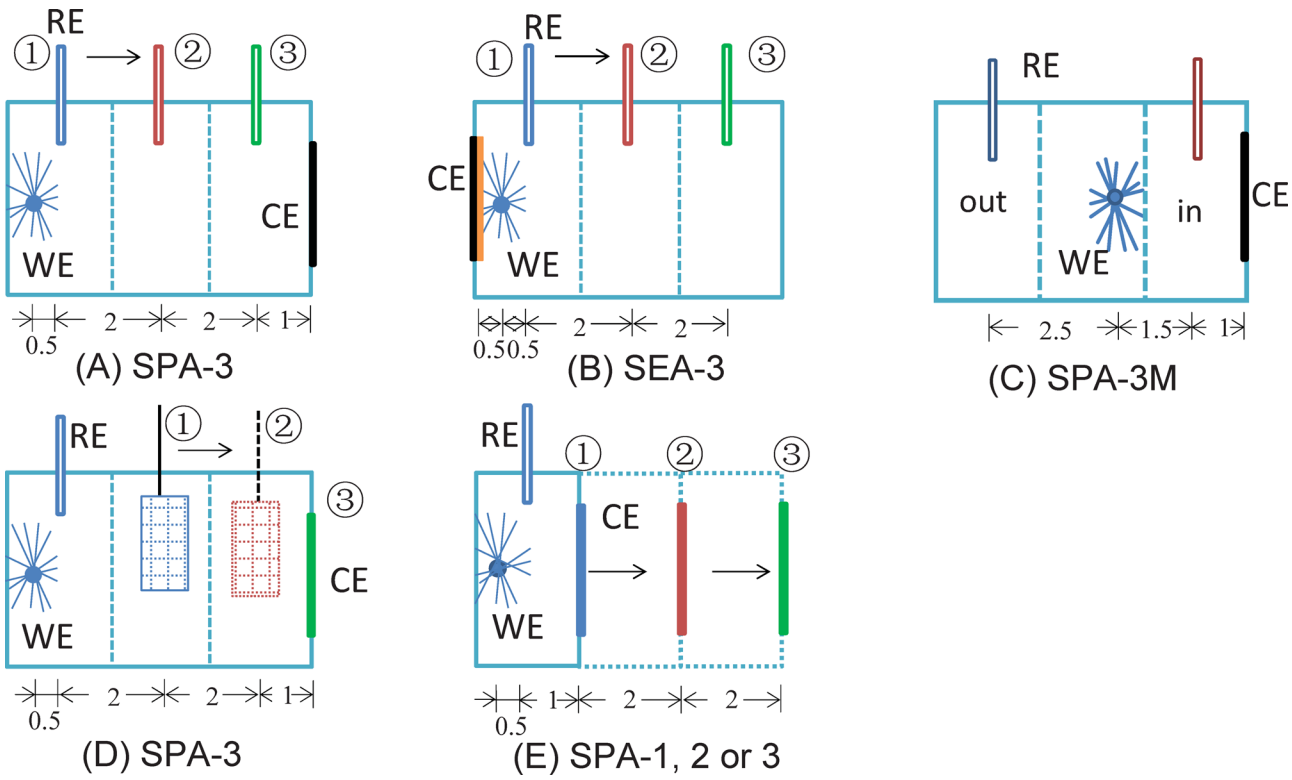

Figure 1. Reactor configurations used to examine the electrode position effect on electrochemical characterization of bioanodes: (**A**) SPA constructed using three 2 cm-cubes with changes of RE positions; (**B**) SEA constructed using three 2 cm-cubes with changes of RE positions; (**C**) SPA with the brush in the middle cube and various RE positions; (**D**) SPA constructed using three 2 cm-cubes, with Pt mesh at various positions or the cathode as the CE; and (**E**) SPA with 1–3 cubes to have various cathode (CE) positions. The numbers below each reactor configuration indicate electrode distances in cm.

distance from the brush core), 2 (in the middle segment, 2.5 cm from the brush core), and 3 (farthest, 4.5 cm from the brush core) during the experiments. The physical spacing between the RE and the anode for each position were kept the same for the SPA-3 and SEA-3 MFCs, to examine the effect of reactor configuration on the measurements. When the RE was inserted in the cube that had the brush anode, the frit was ~3 mm away from the brush edge. The height of the RE in the chamber was kept constant for all the reactors and all placements.

In order to exclude any variations due to differences in anode performance, the SPA-3 MFCs were modified to have the brush anode in the middle cube (SPA-3M, brush core 2.5 cm away from the cathode, Fig. 1C), so that the RE could be placed on either side of the brush. This configuration allowed for a direct comparison of the same anode with different RE positions.

Based on the SPA configuration, the effect of the CE position was examined by two approaches, using both fixed anode and fixed RE positions. In the first approach, three segments were always used so that the electrode spacing between the anode and the cathode was fixed. A piece of Pt mesh at various positions or the cathode was used as the CE during the electrochemical tests (Fig. 1D). CV tests were performed in three successive cycles. In the second approach, the cathode was used as the CE and the position was adjusted by changing the number of cube segments from one to three (SPA1-3, Fig. 1E). MFCs were originally acclimated to SPA-1 for 3 months. After reassembling the reactors with more cube segments, they were operated for 1 week in the SPA-2 configuration, and then for 2 weeks in the SPA-3 configuration before CV tests were performed, allowing time for the anode biofilms to acclimate to the different electrode conditions.

Electrochemical Tests

Electrochemical tests were all performed with anodes as the WE and cathodes as the CE (except as noted) using a potentiostat (VMP3, BioLogic, Knoxville, TN). EIS tests were conducted at anode polarized (apparent) potentials of −0.2 and −0.15 V versus SHE, over a frequency range of 100 kHz to 5 mHz with a sinusoidal perturbation of 10 mV amplitude. The spectra were fitted into an equivalent circuit (Fig. 2A) using the EC-Lab V10.23 software to obtain the uncompensated ohmic resistance (R_u), charge transfer resistance (R_{ct}), and diffusion resistance (R_d). In order to avoid issues related to calculated changes in the R_{ct} and R_d with the given circuit model, we report the combined reaction resistance (R_{rxn}) which is the sum of R_{ct} and R_d. The R_u can also be estimated

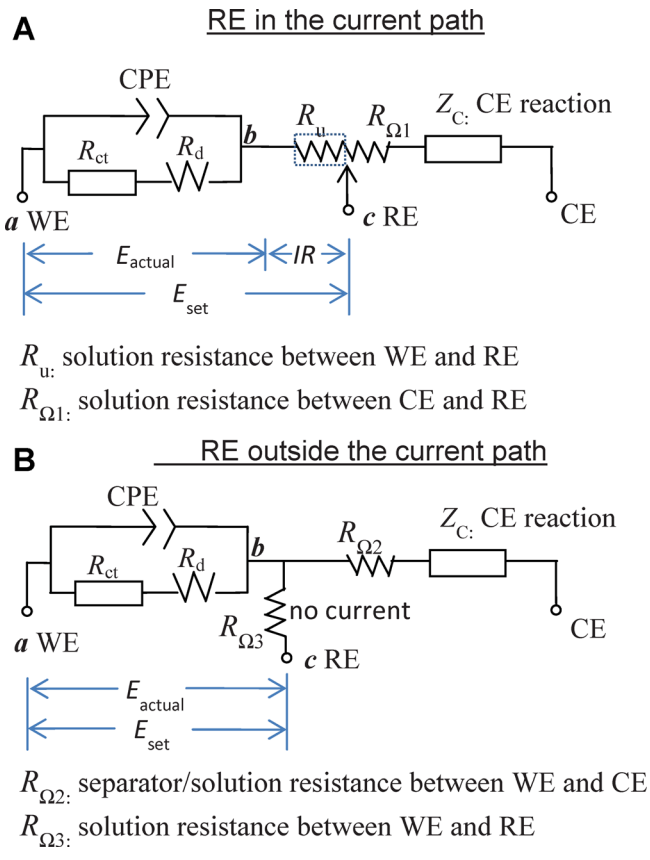

Figure 2. Simplified schematic circuit for the three-electrode setup with: (**A**) RE in the current path; (**B**) RE outside the current path.

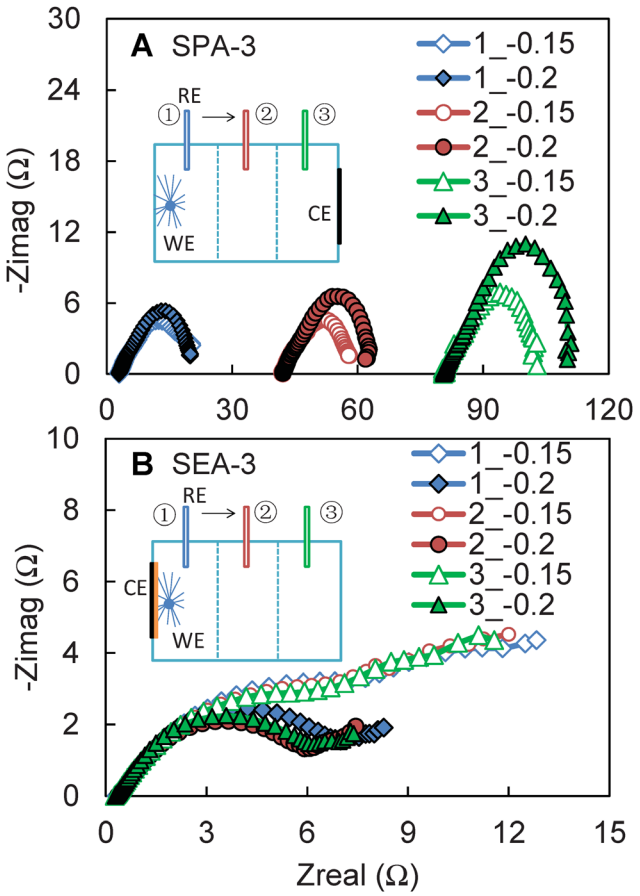

Figure 3. Impact of RE positions on EIS spectra for (**A**) SPA-3 and (**B**) SEA-3, at a set anode potential of −0.2 V (solid symbols) or −0.15 V (open symbols).

by the interception with the Z_{real} axis, and the R_{rxn} be estimated by the diameter of the semicircle in the Nyquist plot.

For CV tests, anode potentials were scanned from −0.49 to +0.31 V (vs. SHE) at a slow scan rate of 1 mV s^{-1}. Experiments were conducted without and with auto IR compensation (ZIR in BioLogic potentiostat, 85% of compensation based on the average of 4 measurements at 100 kHz), which is used to compensate for the IR drop based on the ohmic resistance obtained in high frequency impedance tests. CV tests were repeated four times, and the last cycle, which was comparable to the third cycle, was plotted for these comparisons.

Results and Discussion

Impact of Reactor Configurations and RE Positions using EIS

The EIS spectra showed different responses to the RE position for both the SPA-3 and SEA-3 configurations. With the SPA-3 configuration, the spectra produced were dependent on the RE position (Fig. 3A). The ohmic resistance substantially increased from $R_u = 3 \pm 1$ to $80 \pm 1\ \Omega$ when the RE was moved away from the WE. This ohmic resistance was independent of the polarized potential on the anode, which was consistent with previous tests and our expectations that different set WE potentials should not affect R_u (Zhang et al., 2011). The measured reaction resistance was a function of both the anode polarized potential and the RE position. With the anode set at a potential of −0.2 V, the reaction resistance increased from $R_{rxn} = 17 \pm 2$ to $31 \pm 3\ \Omega$ when increasing the spacing between the WE and the RE (moving from position $1 \rightarrow 3$, Fig. 4A, Supplementary Fig. S1A). When the anode potential was increased to −0.15 V, the reaction resistance did not substantially vary among for the three different positions, with values of $R_{rxn} = 21 \pm 2\ \Omega$ (position 1), $17 \pm 0.2\ \Omega$ (position 2), and $24 \pm 2\ \Omega$ (position 3) (Fig. 4A, Supplementary Fig. S1A). The R_{rxn} was also estimated using the circle fitting method (Hutchinson et al., 2011), and that method produced similar results to the R_{rxn} obtained by this equivalent circuit method (data not shown).

With the SEA-3 configuration, EIS spectra were independent of the RE position (Fig. 3B). The ohmic resistance was $R_u = 0.4 \pm 0.1\ \Omega$ for all three RE positions, and it was much smaller than that obtained for the SPA-3 configuration

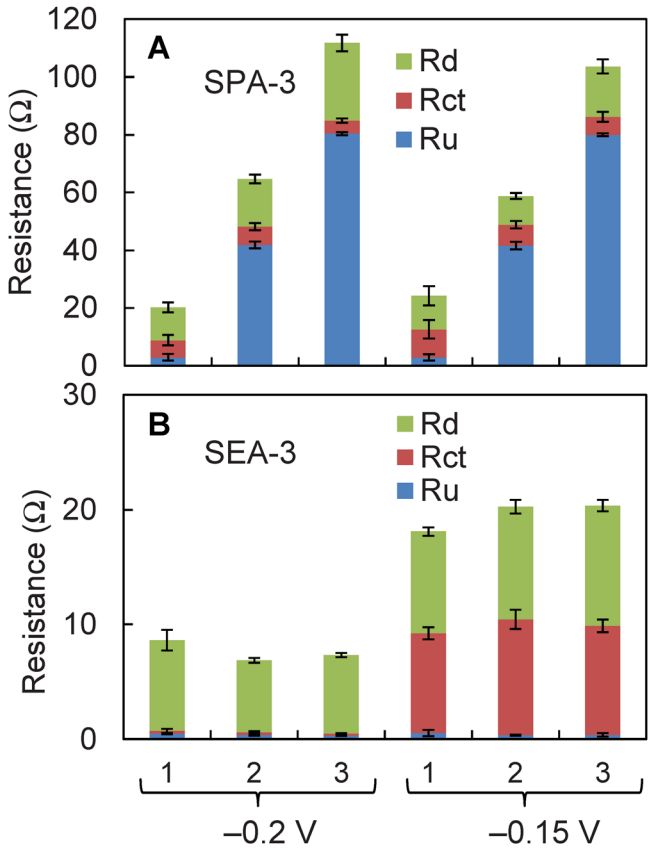

Figure 4. Resistance component analysis of (**A**) SPA-3 and (**B**) SEA-3, using the equivalent circuit described in Figure 2A. The reaction resistance R_{rxn} was the sum of R_{ct} and R_d. (Error bars based on tests with triplicate reactors.) Direct comparisons of R_{rxn} excluding the R_u were shown in Supporting Information as Figure S1.

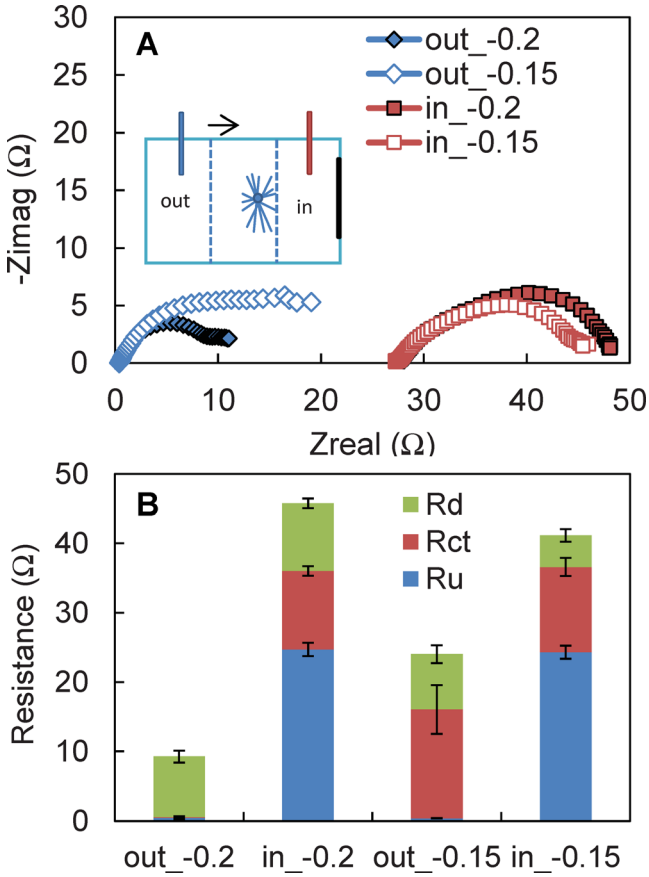

Figure 5. **A**: Nyquist plots of anode EIS spectra at set anode potentials of −0.2 and −0.15 V, with the RE either placed either inside or outside the current path, using the SPA-3M configuration. **B**: Component analysis of the resistances by fitting EIS spectra to the equivalent circuit described in Figure 2A. The reaction resistance R_{rxn} was the sum of R_{ct} and R_d. (Error bars based on triple tests with triplicate reactors.) Direct comparisons of R_{rxn} excluding the R_u were shown in Supporting Information as Figure S2.

(3–80 Ω) with the same physical spacing between the WE and the RE. The kinetic parameters were still affected by the polarized potential on the anode, but not the RE position. The R_{rxn} was $7 \pm 1\,\Omega$ with an anode potential of −0.2 V, and it increased to $R_{rxn} = 19 \pm 1\,\Omega$ at −0.15 V (Fig. 4B, Supplementary Fig. S1B).

In order to directly compare the effect of the RE position on the electrochemical characterization of the same anode (avoiding possible changes in microbiological characteristics by minimizing time between measurements), the SPA-3 reactor was modified so that the brush was moved into the middle of the reactor. In this SPA-3M configuration, the RE could be placed either in between the electrodes, similar to that in the SPA-3, or outside the current path, similar to that in the SEA-3. The RE positions in these tests not only affected the values of the impedance, but they also altered the spectra (Fig. 5A). The difference in shape of the spectra with various RE positions was similar to those observed between the SPA-3 and SEA-3 configurations. The ohmic resistance was $R_u = 0.4 \pm 0.03\,\Omega$ when the RE was outside the current path, compared to $24 \pm 1\,\Omega$ with the RE in the current path. This difference in R_u was consistent with previous results that R_u was much smaller in the SEA-3 than in the SPA-3 configuration. With the RE outside the current path, the reaction resistance substantially increased from $R_{rxn} = 9 \pm 1$ to $24 \pm 4\,\Omega$ when increasing the anode potential from −0.2 to −0.15 V. However, when the RE was placed in the current path, R_{rxn} decreased from $21 \pm 1\,\Omega$ (−0.2 V) to $17 \pm 2\,\Omega$ (−0.15 V) (Fig. 5B, Supplementary Fig. S2). This variation with the RE position was consistent with previous studies that impedance results were a function of the RE position (Fiaud et al., 1987).

Analysis of the Three-Electrode Setup using Schematic Circuits

The changes in resistances with the different reactor configurations and RE placement can be understood in terms of conventional electrical analysis if there are no microbiological changes due to these changes. When no current is drawn from the RE, the current distribution is

determined by the positions of the WE (anode) and the CE (cathode). When the RE is placed between the cathode and the anode, it is in the current path. The position of the RE in the solution divides the total electrolyte resistance between the anode and the cathode into two parts: R_u (between the RE and the anode) and the $R_{\Omega 1}$ (between the RE and the cathode) (Fig. 2A). With the three-electrode setup, the potential difference is set between the anode (point *a*) and the RE (point *c*), thus only R_u is the ohmic resistance that is measured at high frequency. The magnitude of R_u changes in response to the RE position when the RE is in the current path. During the anode EIS tests with a set anode potential, a constant potential difference is set to polarize the anode, in addition to the added sinusoidal perturbation (between *a* and *c*) (Fig. 2A). However, the actual applied potential across the anode/anolyte interface (between point *a* and *b*) deviates from the desired set value due to the IR drop across the R_u ($E_{actual} = E_{set} \pm IR_u$). As the reaction kinetics are affected by the actual applied potential on the WE, R_{rxn} will vary with the RE positions when the RE is placed in the current path, consistent with the experimental results in the SPA-3 configuration.

As current flows between the WE (anode) and the CE (cathode), when the RE is placed on one side of the electrodes and near the WE, the RE is outside the current path and in the electrolyte region that does not have ionic current flow (inactive electrolyte region). This is the situation for the SEA-3 configuration. There are two ohmic resistances in the circuit, with $R_{\Omega 2}$ the ohmic resistance between the cathode and the anode, and $R_{\Omega 3}$ the solution resistance between the anode and the RE (Fig. 2B). As there is no current flow in the electrolyte between the anode and the RE (inactive region), $R_{\Omega 3}$ will not cause a potential drop, making points *b* and *c* equipotential. Changes in RE positions in the inactive region will result in the changes of the $R_{\Omega 3}$, but this will not affect the IR drop and the actual applied potential to the anode (Fig. 2B). When a constant potential difference was set between the anode (*a*) and the RE (*c*) for the SEA-3, the actual applied potential (between *a* and *b*) had little deviation from the set value (between *a* and *c*). Therefore in the experiments with the SPA-3 configuration, the R_u was small (0.4 Ω) and independent of the physical spacing between the RE and the anode, and the measured reaction resistance R_{rxn} did not change with RE positions (Figs. 3B and 4B). As the magnitude of the R_u indicates the magnitude of potential drop between the location of the RE to the WE surface (Hsieh et al., 1997), the RE position-independent R_u of 0.4 Ω in the SEA-3 configuration suggested that the inactive electrolyte region was an equipotential volume.

Effect of IR Compensation on CV Tests

In voltammetry tests, ohmic resistance between the RE and WE can affect the resulting spectra. This is why it is recommended that the RE be placed as close as possible to the WE. To exclude the effects of the ohmic resistance on CVs, most potentiostats have software settings that can be used to compensate for this IR drop during scans. It is not clear from many bioelectrochemical studies, however, that this IR correction is used. In our tests, when R_u were found to be small compared to the reaction resistances, as in the case of the SEA-3 results, the voltammograms were independent of the RE position without the IR compensation (Supplementary Fig. S3). In this configuration, the use of IR compensation is therefore not essential for interpreting the results. However, in the SPA-3 setup, with the RE far away from the anode, IR compensation must be used. When the CV tests were conducted without the auto IR compensation, both the peak current and the shape of the voltammograms varied with the RE position (Fig. 6A). The IR drop not only caused errors on the actual applied anode potential ($E_{actual} = E_{set} \pm IR$), but it also reduced, in a non-linear manner, the effective scan speed during the measurement due to the change of produced current. When the RE was placed in position 3, which had the largest distance from the WE, the electrolyte resistance was dominant (80 Ω), resulting in overlap in the forward and reverse scans. With the auto IR compensation used in CV tests, the voltammograms were generally independent of the RE positions (Fig. 6B) even with a large distance between the anode and the RE. Therefore it is

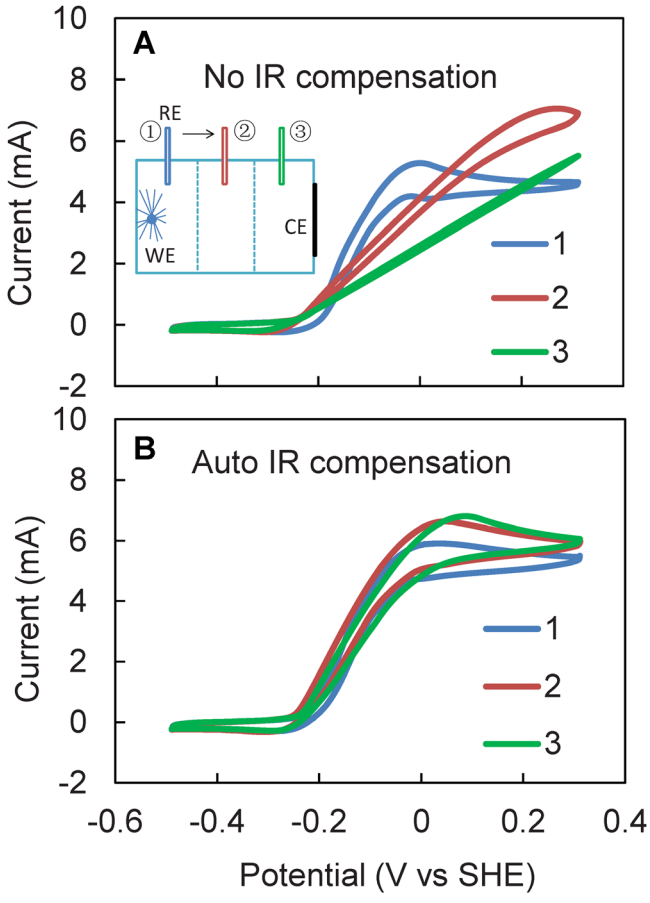

Figure 6. CVs of anodes with different RE positions in the SPA-3 configuration: (**A**) no IR compensation; (**B**) auto IR compensation.

important to compensate for the IR drop in tests when the uncompensated electrolyte resistance is large compared to the WE resistance.

Even with IR compensation, there were still noticeable differences in the CVs when the RE was placed inside or outside the current path in the SPA-3M configuration. When the RE was placed outside the current path, the voltammogram showed apparently faster kinetics (angled towards more negative potentials) than those obtained inside the current path at similar peak current values (Fig. 7A). In the first derivative CV (DCV) plot, the midpoint potential was more clearly identified when the RE was outside of the current path, and the value was more negative relative to that obtained with the RE inside the current path (Fig. 7B). The difference in the CVs even with IR compensation could be due to the insufficient compensation by the potentiostat, or more likely a non-uniform current distribution in the electrolyte between the anode and the cathode. In our tests, the IR compensation was set at 85%, and the R_u measured before the CV tests could also vary during the tests. When the RE was placed in the current path, the RE was large enough to sample a range of equipotential surfaces and thus an average potential. Therefore, errors were introduced into the CVs and EIS results with the RE inside the current path. When the RE was placed outside the current path, the potential was more uniform and there was only a small IR drop, making the measurements more reliable in this location.

Impact of CE Positions

The variation in the CE position may not affect the electrochemical responses of the system, but it can produce actual changes in the microbial communities and therefore alter bioanode performance. To demonstrate that such changes occur, two different types of experiments were done to distinguish electrochemical responses from biological ones. In this first set of tests, using the SPA configuration and fixed anode and RE positions as shown in Figure 8A, a Pt mesh electrode was used as the CE. When the CE was moved away from the anode (position 1 and 2), or the cathode was

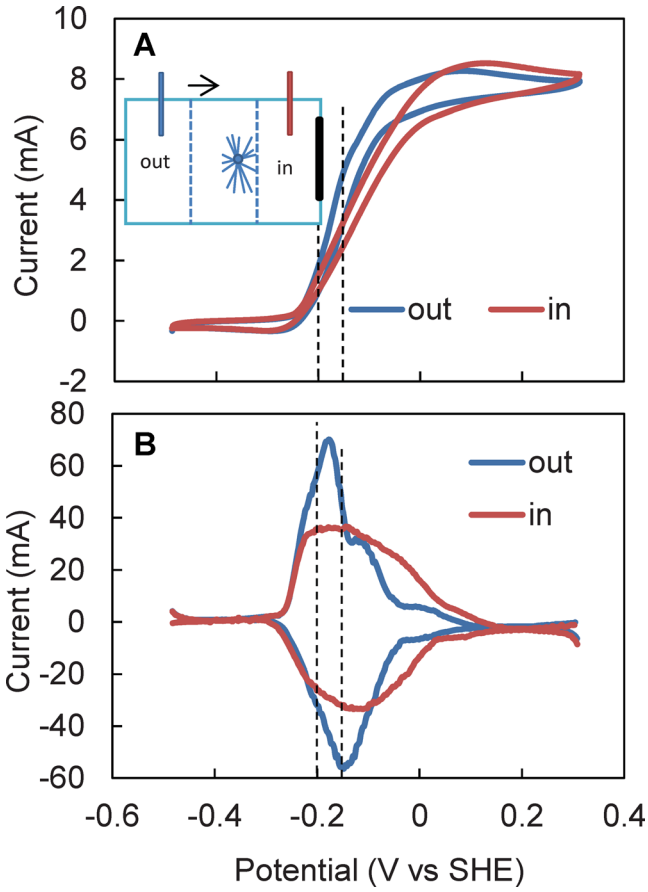

Figure 7. **A**: Anode CVs and (**B**) first derivative of CVs with the RE placed inside or outside of the current path, using the SPA-3M configuration. (Dashed lines indicate the potentials where EIS tests were conducted). Both CVs were obtained with auto IR compensation at a slow scan rate of 1 mV s^{-1}.

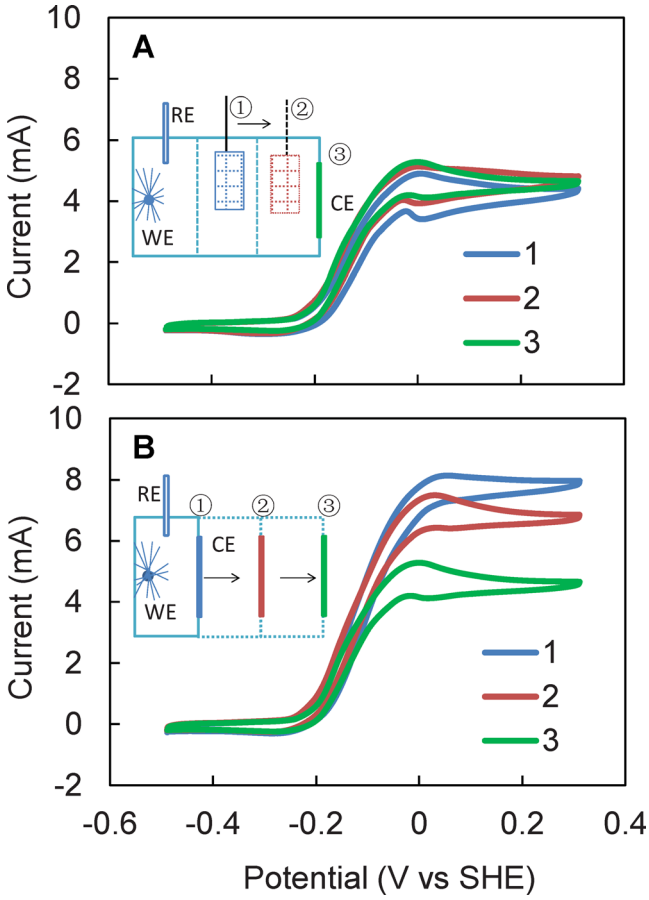

Figure 8. The effect of CE position on the anode CVs. **A**: When a platinum mesh was used as the CE, there was little change in the CVs when the CE was moved away from the WE (positions 1 to 2), or with the cathode as the CE and no Pt mesh (position 3). Note that the cathode was kept in place for the position 1 and 2 tests. **B**: Here the cathode was the CE, and it was moved into different positions by changing the reactor to be longer, resulting in noticeable changes in the CVs due to changes in the biofilm properties.

used as the CE (position 3), the anode CVs showed only minor changes. This independence of the CV results with the change of CE position/type is expected based on only the electrochemistry changes, as the CE distance should not affect the electrochemical response of the system (Bard and Faulkner, 2001).

In the second set of tests, the cathode was moved away from the anode by adding more cube segments to the reactor. The disassembling and reassembling of the reactor, and refilling the medium required more time than in the first set of tests, and therefore MFCs were allowed to acclimate for several cycles to allow for stable changes in the biofilm using a constant external resistance of 1,000 Ω. As a result of this procedure which allowed time for biofilm acclimation to a different set condition, the anode CV peak current decreased from 8.1 to 5.3 mA (Fig. 8B). This decrease in peak current had to be a true change in the anode performance that was due to the biological response to the change in the cathode (CE) position relative to the anode, as there is no appreciable change in the electrochemical response as shown by the first series of tests where there was insufficient time for microbial adaptation to the different working conditions. When the cathode was moved away from the anode in this second set of tests, the produced current decreased as a result of the increased electrode spacing and higher internal resistance. The anode biofilm therefore became acclimated to this lower anode potential to produce lower current and changed its activity in response to the operating conditions, making the resulting CVs dependent on the CE (cathode) positions. This demonstrated that changes that alter anode potentials, such as introducing additional resistances between the electrodes, can alter both electrochemical and biological responses of the system.

Conclusions

A three-electrode arrangement requires careful consideration from both electrochemical and biological perspectives to characterize and make accurate comparisons of bioelectrodes. From the results obtained here, it is recommended that the RE be placed outside the current path and near the WE, where potential distribution is uniform and there is only a small IR drop. This RE placement will result in more consistent measurement of kinetic parameters, although it eliminates the ability to correctly measure the solution resistance. As this RE placement allows a more accurate set potential, it will not alter the bioelectrochemical performance of the biofilms through inadvertent changes in applied potentials. When the RE has to be placed in the current path, the position should be as close as possible to the WE to minimize the IR drop. When the electrolyte ohmic resistance is significant compared to the WE resistance, IR compensation is necessary to obtain accurate results. Although the CE distance from the WE may not affect the characterization electrochemically, the position of CE still requires attention as changing it may result in biological changes in performance of the bioelectrode after acclimation.

The authors thank David Jones for help with the experiments, Dr. Justin Tokash from Los Alamos National Laboratory, and Bill Eggers from BioLogic for useful discussions. This research was supported by Award KUS-I1-003-13 from the King Abdullah University of Science and Technology (KAUST).

References

Bard AJ, Faulkner LR. 2001. Electrochemical methods: Fundamentals and applications. New York: John Wiley & Sons.

Chen G, Zhang F, Logan BE, Hickner MA. 2013. Poly(vinyl alcohol) separators improve the coulombic efficiency of activated carbon cathodes in microbial fuel cells. Electrochem Commun 34(0):150–152.

Cheng S, Liu H, Logan BE. 2006. Increased performance of single-chamber microbial fuel cells using an improved cathode structure. Electrochem Commun 8:489–494.

Dumas C, Basseguy R, Bergel A. 2008. Electrochemical activity of Geobacter sulfurreducens biofilms on stainless steel anodes. Electrochim Acta 53 (16):5235–5241.

Fan Y, Hu H, Liu H. 2007. Enhanced coulombic efficiency and power density of air-cathode microbial fuel cells with an improved cell configuration. J Power Sources 171(2):348–354.

Fiaud C, Keddam M, Kadri A, Takenouti H. 1987. Electrochemical impedance in a thin surface electrolyte layer. Influence of the potential probe location. Electrochim Acta 32(3):445–448.

Hack HP, Moran PJ, Scully JR. 1990. Influence of electrolyte resistance on electrochemical measurements and procedures to minimize or compensate for resistance errors. In: Scribner LL, Talylor SR, editors. The measurement and correction of electrolyte resistance in electrochemical tests. Philadephia: ASTM. p 5–26.

Hays S, Zhang F, Logan BE. 2011. Performance of two different types of anodes in membrane electrode assembly microbial fuel cells for power generation from domestic wastewater. J Power Sources 196(20):8293–8300.

He Z, Mansfeld F. 2009. Exploring the use of electrochemical impedance spectroscopy (EIS) in microbial fuel cell studies. Energy Environ Sci 2 (2):215–219.

He Z, Wagner N, Minteer SD, Angenent LT. 2006. The upflow microbial fuel cell with an interior cathode: Assessment of the internal resistance by impedance spectroscopy. Environ Sci Technol 40(17):5212–5217.

Hsieh G, Mason TO, Garboczi EJ, Pederson LR. 1997. Experimental limitations in impedance spectroscopy: Part III. Effect of reference electrode geometry/position. Solid State Ionics 96(3–4):153–172.

Hutchinson AJ, Tokash JC, Logan BE. 2011. Analysis of carbon fiber brush loading in anodes on startup and performance of microbial fuel cells. J Power Sources 196(22):9213–9219.

Liu H, Logan BE. 2004. Electricity generation using an air-cathode single chamber microbial fuel cell in the presence and absence of a proton exchange membrane. Environ Sci Technol 38(14):4040–4046.

Logan BE, Aelterman P, Hamelers B, Rozendal R, Schröder U, Keller J, Freguiac S, Verstraete W, Rabaey K. 2006. Microbial fuel cells: Methodology and technology. Environ Sci Technol 40(17):5181–5192.

Logan BE, Cheng S, Watson V, Estadt G. 2007. Graphite fiber brush anodes for increased power production in air-cathode microbial fuel cells. Environ Sci Technol 41(9):3341–3346.

Logan BE, Rabaey K. 2012. Conversion of wastes into bioelectricity and chemicals by using microbial electrochemical technologies. Science 337 (6095):686–690.

Lovley DR. 2006. Bug juice: Harvesting electricity with microorganisms. Nat Rev Microbiol 4:497–508.

Lovley DR. 2008. The microbe electric: Conversion of organic matter to electricity. Curr Opin Biotechnol 19(6):564–571.

Marsili E, Rollefson JB, Baron DB, Hozalski RM, Bond DR. 2008. Microbial biofilm voltammetry: Direct electrochemical characterization of catalytic electrode-attached biofilms. Appl Environ Microbiol 74(23): 7329–7337.

Piela P, Springer TE, Davey J, Zelenay P. 2007. Direct measurement of iR-free individual-electrode overpotentials in polymer electrolyte fuel cells. J Phys Chem C 111(17):6512–6523.
Rabaey K, Clauwaert P, Aelterman P, Verstraete W. 2005. Tubular microbial fuel cells for efficient electricity generation. Environ Sci Technol 39 (20):8077–8082.
Sun D, Call DF, Kiely PD, Wang A, Logan BE. 2012. Syntrophic interactions improve power production in formic acid fed MFCs operated with set anode potentials or fixed resistances. Biotechnol Bioeng 109(2):405–414.
Torres CI, Krajmalnik-Brown R, Parameswaran P, Marcus AK, Wanger G, Gorby YA, Rittmann BE. 2009. Selecting anode-respiring bacteria based on anode potential: Phylogenetic, electrochemical, and microscopic characterization. Environ Sci Technol 43(24):9519–9524.
Wagner RC, Call DF, Logan BE. 2010. Optimal set anode potentials vary in bioelectrochemical systems. Environ Sci Technol 44(16):6036–6041.
Wang X, Feng Y, Ren N, Wang H, Lee H, Li N, Zhao Q. 2009. Accelerated start-up of two-chambered microbial fuel cells: Effect of anodic positive poised potential. Electrochim Acta 54(3):1109–1114.
Wei J, Liang P, Cao X, Huang X. 2010. A new insight into potential regulation on growth and power generation of geobacter sulfurreducens in microbial fuel cells based on energy viewpoint. Environ Sci Technol 44 (8):3187–3191.
Winkler J, Hendriksen PV, Bonanos N, Mogensen M. 1998. Geometric requirements of solid electrolyte cells with a reference electrode. J Electrochem Soc 145(4):1184–1192.
Zeng R, Slade RCT, Varcoe JR. 2010. An experimental study on the placement of reference electrodes in alkaline polymer electrolyte membrane fuel cells. Electrochim Acta 56(1):607–619.
Zhang F, Merrill MD, Tokash JC, Saito T, Cheng S, Hickner MA, Logan BE. 2011. Mesh optimization for microbial fuel cell cathodes constructed around stainless steel mesh current collectors. J Power Sources 196 (3):1097–1102.
Zhang F, Xia X, Luo Y, Sun D, Call DF, Logan BE. 2013. Improving startup performance with carbon mesh anodes in separator electrode assembly microbial fuel cells. Bioresour Technol 133(0):74–81.
Zhu X, Tokash JC, Hong Y, Logan BE. 2013. Controlling the occurrence of power overshoot by adapting microbial fuel cells to high anode potentials. Bioelectrochemistry 90(0):30–35.

Supporting Information

Additional supporting information may be found in the online version of this article at the publisher's web-site.